Journal of Engineering Science 13(2), 2022, 127-137
DOI: https://doi.org/10.3329/jes. v13i2.63733

JES
an international Journal

REMOTE SENSING TECHNIQUES AS A TOOL FOR ENVIRONMENTAL MONITORING IN AND AROUND OF RAJBANDH LANDFILL AT KHULNA CITY

Emruz Arafat[1*] and Islam M. Rafizul[2]

[1] *student, Department of Civil Engineering, Khulna University of Engineering & Technology, Bangladesh*
[2]*Professor, Department of Civil Engineering, Khulna University of Engineering & Technology, Bangladesh*

Received: 13 February 2022 Accepted: 18 December 2022

ABSTRACT

Uncollected trash in the streets and other public areas, trash placed without regard for drainage systems, and trash that has contaminated water sources near uncontrolled dumps all contribute to a hazardous environment and public health situation in Khulna. The Batiaghata thana area, which contains the Rajbandh dump, was analyzed by computing the LST, NDVI, SAVI, and MSAVI. From a low of 23.00°C in 1995, the Batiaghata thana is predicted to reach a high of 41.43°C by 2020, courtesy of the Long Term Observational Dataset (LST). According to the NDVI results, the proportion of 'Bare Soil' in Batiaghata thana increased substantially from 1.20 percent to 4.57 percent, and the percentage of 'Structural Object' climbed from 1.25 percent to 23.06 percent. From 1995 to 2000, the maximum MSAVI value increased from 0.76 to 0.80. Results indicate that inappropriate waste management at the Rajbandh dump negatively affected local ecosystems.

Keywords: *Waste landfill, Landfill monitoring; remote sensing indices, Khulna*

1. INTRODUCTION

The output of municipal solid trash has increased as a result of a combination of factors, including the quickening rate of population growth, the broadening scope of economic activity (such as urbanization and industrialization), and the enhancement of living standards. As of the 20th of April in 2015, the overall population of Bangladesh was 158.36 million people. (Population of Bangladesh, 2019) Based on population density, Bangladesh is the fifth most, where 1015 persons live per sq. km. (Population of Bangladesh, 2019). Environmental monitoring is an essential component of the natural science curriculum and strategic planning of any nation. Any plan that lacks strategic environmental monitoring has the danger of failing and being uneconomical. By conducting effective environmental monitoring, we may correlate a polluting source with its source. Population development and the expansion of economic activities, such as urbanization, industrialisation, and improved living conditions, have contributed to an increase in municipal solid waste production. Municipal waste management has long been a point of dispute for local governments around the world, especially in regards to garbage disposal. Each year, the globe produces 1,3 billion metric tons of municipal solid waste (MSW). This number is increasing daily. By 2025, trash generation is predicted to reach 2.2 billion tons. (Kawai, 2016) The practice of gathering data about one's surroundings via the use of technology is known as remote sensing. This may be achieved by detecting and collecting any energy that is reflected or emitted, as well as analyzing, assessing, and applying the data that is collected. The energy that is reflected off the Earth is measured by remote sensors in order to get information. Both satellites and aircraft are viable options for mounting these sensors. Khulna is an important industrial and port city in Bangladesh and is the country's third-largest metropolitan center. The town's population grew significantly as a direct result of the rise of economic and financial activities, which led to an increase in employment opportunities. As a direct consequence of this, the quantity of solid waste that is produced has risen in step with the expansion of the human population. There is a demonstration sanitary landfill located at Rajbandh, Khulna (Rafizul, Spatiality, seasonality and index analysis of heavy metals in soil of waste disposal site in Khulna of Bangladesh, 2019) The landfill is a reactor that improves the decomposition process. It requires an advanced monitoring system to minimize the environmental impact of waste received by the landfill and for a better waste management system. There are several environmental parameters which should be monitored to ensure that it doesn't have any significant negative impact on the environment. Environmental monitoring of a landfill can be achieved by both in-situ method and remote sensing data (Danthurebandara M., 2012). The study's main goals are to observe the temperature distribution and vegetation health condition at the Rajbandh landfill site and the surrounding region utilizing ArcGIS, and to evaluate the current status of waste management at the Rajbandh landfill site of Khulna.

*Corresponding Author:emruz10826@gmail.com

ISSN 2075-4914 (print); ISSN 2706-6835 (online)

2. MATERIALS AND METHODS

The approach of the study requires collecting the LST, NDVI, SAVI, and MSAVI from the Batiaghata subdistrict area, which covers the Rajbandh dump in its scope of coverage. In order to graphically represent the methodological procedure that was followed in the course of conducting this research, a flow diagram was utilized. The following section offers a concise summary of the research approach that was utilized in this particular investigation: Figure 1 provides a detailed overview of the process of the approach that is being used.

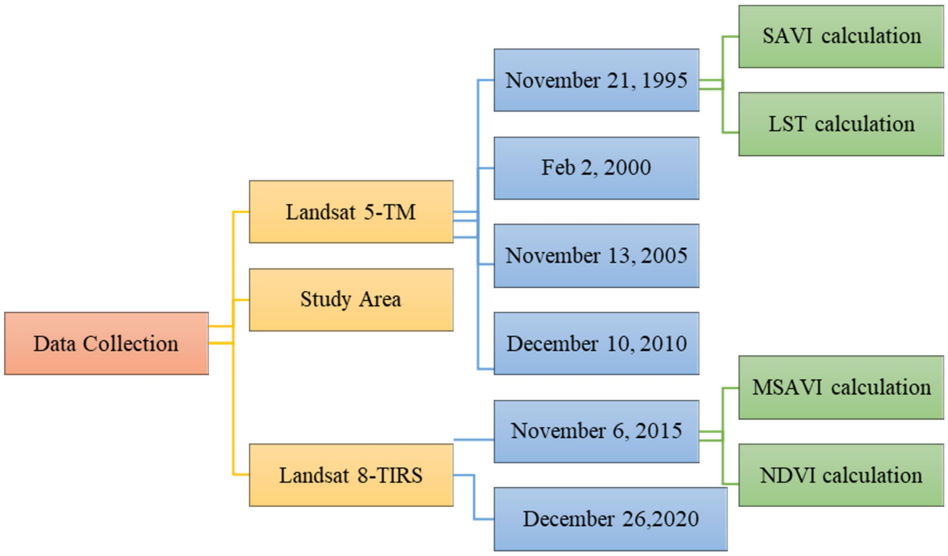

Figure 1: Flow chart of Methodology

2.1 Study Area

The dumping system for municipal solid waste (MSW) is divided into two parts: open dumping and sanitary landfill. Sanitary landfill is one of the most important and secure facilities for the disposal of MSW. A pilot scale sanitary landfill is in Rajbandh Khulna, 8 kilometres from the city centre, on the north side of the Khulna-Satkhira highway. Rajbandh, which is located in Khulna, Bangladesh, was chosen as the research region, and its position may be seen in Figure 2.

2.2 Data Collection

The Rajbandh landfill has been in operation since 1984. Because the major goal of this study is to document the Rajbandh landfill's environmental impact from the beginning, photos taken at 5-year intervals from 1995 to 2020 were used. The US Geological Survey (USGS) maintains webpages at www.glovis.usgs.gov and www.earthexplorer.usgs.gov, both of which offer free downloads of the Landsat data. The numbers 137 and 44 correspond to the row and the route, respectively. The data was analysed with ArcGIS. Bangladesh Agricultural Research Council provided the shape file for Batiaghata thana (BARC).

2.3 Remote Sensing Indices

During our research, we make use of remote sensing indices such as NDVI, SAVI, MSAVI, and LST for the purpose of environmental monitoring at and in the vicinity of the Rajbandh Landfill site.

2.3.1 NDVI

By evaluating remote sensing data, the normalized difference vegetation index (NDVI) facilitates the identification of green vegetated boundaries and their conditions. Visible as RGB (Red, Green, and Blue) and near-infrared wavelengths have very different absorption and reflection characteristics. In visible light (from 0.4 to 0.7 m), vegetated edges seem dark; but, in near-infrared wavelengths (from 0.7 to 1.1 m), vegetated areas appear brilliant. By integrating this distinction, naturally occurring green vegetated limits can be determined.

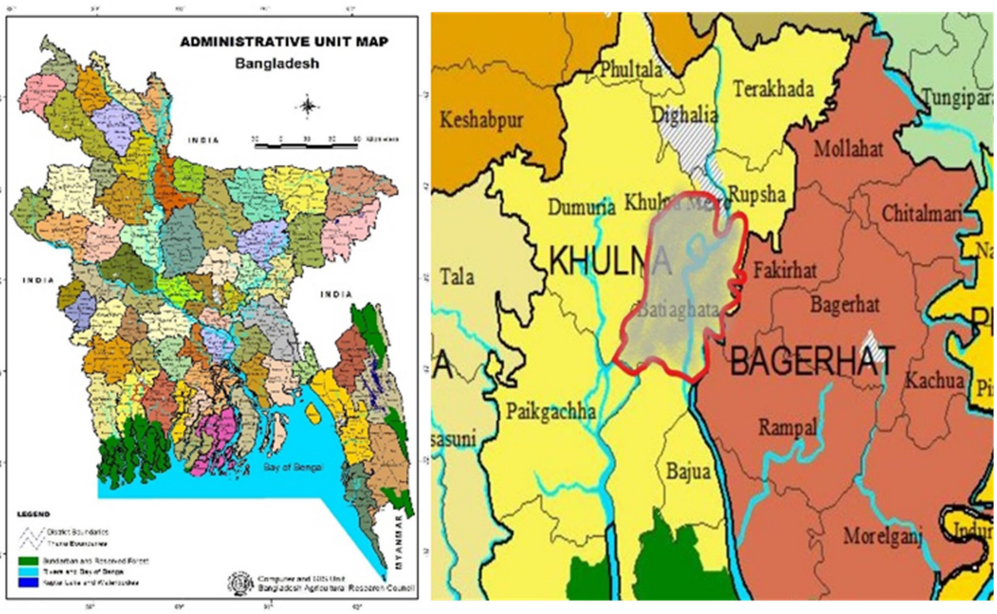

Figure 2: Map showing selected location of study area at Rajbandh, Khulna, Bangladesh (Location: Latitude: 22º47'43.17'', Longitude: 89º29'58.35").

Green trees absorb solar radiation in the area of photosynthetically active radiation (PAR), which is utilized to generate energy during photosynthesis. Because organic particles may be produced at wavelengths shorter than approximately 700 nanometers, leaf cells can re-transmit solar radiation in the near-infrared region, where 50% of the total solar energy is conducted. This absorption mechanism occasionally damages the green trees' tissues by warming them. Therefore, vegetation boundaries seem darker in the PAR spectrum and brighter in the near-infrared spectrum. More of these wavelengths are absorbed and reflected, causing more leaves to emerge. As a result of this phenomena, leaves absorb visible light and reflect near-infrared wavelengths with great intensity.. (Interpretation of NDVI , 2019) A plant becomes more generative, when it absorbs more visible light. Conversely, when it turns out anhydrous, as well as diseased, it absorbs more near-infrared light. The values of NDVI calculated by using the following Equation 1.

$$NDVI = \frac{(NIR - R\ \ )}{(NIR + Red)} \quad (1)$$

The band reflectance measured in the Red (visible) wavelength is interpreted differently than the band reflectance measured in the near-infrared wavelength. If the amount of reflection in visible wavelengths is substantially smaller than the amount of reflection in near-infrared wavelengths, then the region does not have a significant quantity of green vegetated terrain or forest. Additionally, the Normalized Difference Vegetation Index (NDVI) is a symbol of the photosynthetic capacity to absorb energy. (Range of output value of NDVI, 2019)

2.3.2 SAVI

The Soil-Adjusted Vegetation Index (SAVI) is a vegetation index that attempts to reduce soil brightness dominances by employing a soil reconciliation factor.

When the soil periphery has low (i.e., 40%) plant cover, the reflection of light from the near infrared and red spectrums has an effect on the vegetation index. This issue becomes severe when varied soil types reflect multiple wavelengths of red and near-infrared light. SAVI is enhanced by the modification of NDVI for usage in barren regions with low vegetative cover. A soil reconcilement factor L was added to the NDVI equation to improve the SAVI equation. (Bannari, 1995). The values of SAVI calculated by using the folloing Equation 2.

$$SAVI = \frac{((NIR - Red)}{(NIR + Red + L))} * (1 + L) \quad (2)$$

Where NIR refers to the reflectance value of the near infrared band, Red refers to the reflectance value of the red band, all of which have their own wavelength ranges for a number of Landsats, and L refers to the soil reconcilement factor. In order to achieve optimal reconcilement of the soil impact, the L factor ought to change

in the opposite direction depending on the amount of vegetation already present. The L value varies depending on the density of the surrounding vegetation. L=1 means that there is no green vegetation cover, but L=0 indicates that there is a very high level of vegetation cover.

In addition, regardless of whether or not L is equal to zero, SAVI is always equal to NDVI. Huete utilized a constant L=0.5 despite the fact that this value can compress soil noise several times beneath a significant quantity of green vegetation. This is because this reconcilement factor changes depending on the density of the vegetation. In addition to this, if one were to build an iterative function, reliable measurement of the L value would be possible.. (Huete, 1988) (J. Qi, 1994).

2.3.3 MSAVI

The title MSAVI stands for the "Modified Soil Adjusted Vegetation Index." This index is a version of SAVI that further reduces soil brightness dominances by reinstating the soil reconcilement factor L, which ultimately leads to higher vegetation susceptibility.

MSAVI and SAVI both apply a general Equation 3 to shrink soil brightness influences as follows:

$$SAVI/MSAVI = \frac{(NIR - Red)}{(NIR + Red + L)} * (1 + L) \quad (3)$$

Where NIR stands for the reflectance value of the near infrared band, Red stands for the reflectance value of the red band, and L stands for the soil reconcilement factor.

In SAVI, L is often left unmodified at its default value of 0.5; however, in MSAVI, the soil reconcilement factor may be easily determined through the use of Equation 4:

$$L = 1 - \frac{(2 * s * (\text{NIR} - \text{Red})(\text{NIR} - (s * \text{Red})}{(\text{NIR} + \text{Red})} \quad (4)$$

Where s is the slope of the soil line in a diagram showing red versus near infrared reflectance values. An image's soil line may be determined from the intersection of red and near infrared pixel values, which can be done by plotting red reflectance values against near infrared reflectance values for each pixel in the picture. (Jiang Z., 2007) Compared to other vegetation indices, MSAVI is significantly better at detecting soil noise. In MSAVI, the soil reconcilement factor L works to maximize plant response while simultaneously reducing soil surface deviation. Whether L trends toward zero or not, the MSAVI behaves similarly to the NDVI since L=0 indicates very high vegetation cover. On the other side, when there is no green plant cover (L=1), the MSAVI resembles the PVI or WDVI. Finally, in cases with moderate vegetation cover, the MSAVI is nearly equivalent to the SAVI.. (Huete, 1988). Following the success of the original MSAVI, which was designed to provide more precise data on plant cover, the MSAVI2 was introduced to more readily determine the soil reconcilement factor. Since L is not strictly necessary for the MSAVI2, an iterative L function was implemented in Equation 5.

$$\text{MSAVI2} = \frac{(2(\text{NIR} + 1) - \text{Square Root}((2 * \text{NIR} + 1)\ \hat{}2 - 8(\text{NIR} - \text{Red}))}{2} \quad (5)$$

2.3.4 LST

As the name implies, Land Surface Temperature (LST) is the temperature at which the earth's surface is found. An essential factor in remote sensing, it is used to quantify the amount of energy at the Earth's surface. The significance it plays in assessing global environmental changes using Landsat data remains crucial. (Song Z., 2018).With the improvement of remote sensing, satellite data offer the chance of calculating LST with high temporal resolution rather than ground pointbased values .The Landsat satellite series has more than 30 years of archived thermal infrared imagery from which LST is determined.

Single-channel methods, split-window techniques, and multi-angle methods are just a few of the ways that LST estimates have been calculated using TIR data. These techniques rely on statistical correlations or assumptions and limits to address the retrieval problem, but they aren't without their flaws and require precise correction for atmospheric effects. It is hoped that as spectral, spatial, and temporal resolution continue to advance, an effective approach for simply achieving LST will soon become available.

The energy balance of the Earth depends in part on LST measurement since it regulates surface air temperature and outgoing long-wave radiation. It's one of the most important indicators of total energy resources. Soil moisture, land usage, and plant growth, for instance, all have an impact on how quickly LST changes. Since soil conditions are directly related to plant growth, higher LST indicates less soil moisture or dry soil and potentially sparse plants.

When temperatures rise, precipitation patterns shift, and humidity levels rise and fall, as well as when CO2 and other gases like water vapor have a direct influence, the surface of the land is altered. The global climate is also directly affected by changes in land use, such as urbanization, deforestation, and desertification, which raise surface temperatures and decrease evaporation.

Measurements of LST also play an important role in the study of atmospheric feedbacks, the development of models, the administration of water and crops, the detection and prevention of fires, and the tracking of the hydrological cycle.

Calculating process of LST
a) For Landsat-5
Step-1:

Radiation in the microwave range that escapes Earth's upper atmosphere and is measured as a temperature is known as the brightness temperature (TB). Top of Atmosphere (TOA) spectral radiance (L) was required for location of TB of a region. The TIR band's TB was determined using Equation 6.

$$TB = \frac{K2}{Ln\left((K1 / L\lambda) + 1\right)} \quad (6)$$

Both K1 and K2 may be found in Table 1 below with their respective values:

Table 1: Thermal Constant of Band 6

Thermal Constant	Band 6
K1	607.76
K2	1260.56

where K1 and K2 are thermal conversion constants that shift depending on the TIR spectrum. Upper Atmospheric Spectral Radiance (Lλ) .

Step-2:
The value of Top of Atmospheric (TOA) spectral radiance (Lλ) was determined by thes following Equation 7:

$$L\lambda = \frac{(LMax - LMin)}{(QcalMax - QcalMin)}\left(Qcal - QcalMin\right) + LMin \quad (7)$$

where,
LMax - Radiance Max Band 6 ; LMin - Radiance Min Band 6;QcalMax - Quantize Cal Max Band 6
QcalMin - Quantize Cal Min Band 6;Qcal - Band 6 Image
The values of Metadata are given in the Table 2:

Table 2: Metadata values of Band 6

Metadata	Band 6
LMax	15.303
LMin	1.238
QcalMax	255
QcalMin	1

For Landsat-8:
Step-1:
Radiation in the microwave range that escapes Earth's upper atmosphere and is measured as a temperature is known as the brightness temperature (TB). Top of Atmosphere (TOA) spectral radiance (L) was required for location of TB of a region. The TIR band's TB was determined using Equation 8.

$$TB = \frac{K2}{Ln\left((K1 / L\lambda) + 1\right)} \quad (8)$$

Both K1 and K2 may be found in Table 4 below with their respective values:

Table 3: K1 & K2 Values for Band 10 & 11.

Thermal Constant	Band 10	Band11
K1	1321.08	1201.14
K2	777.89	480.89

where K1 and K2 are thermal conversion constants that shift depending on the TIR spectrum. Upper Atmospheric Spectral Radiance (Lλ).

Step-2:
Multiplying each TIR band by its multiplicative rescaling factor (0.000342) and then adding the additive rescaling factor (0.1), we were able to get the value of TOA spectral radiance (L). Equation 9 was used to calculate the Top-of-Atmosphere (TOA) spectral radiance (L) value:

$$L\lambda = ML * Qcal + AL \quad (9)$$

where,
Lλ - Top of Atmospheric Radiance in watts/ (m2*srad*µm)
ML - Band specific multiplicative rescaling factor (Radiance_multi_band_10/11 for Landsat 8), (Radiance_multi_band_6 for Landsat 5);Qcal - Band 10/ 11 image,
AL - Band specific additive rescaling factor (Radiance add band 10/11 for Landsat 8), (Radiance add band 6 for Landsat 5)
The rescaling factors are given in the Table 4 :

Table 4: Rescaling Factors.

Rescaling Factor	Band 10	Band 11
ML	0.000342	0.000342
AL	0.1	0.1

Step-3:
Finding LST requires first determining the LSE of the area. To calculate LSE, the NDVI threshold approach was applied. The formula for calculating LSE is as follows:

$$LSE = \varepsilon s\,(1 - FVC) + \varepsilon v * FVC \quad (10)$$

where,
εs and εv - soil and vegetative emissivity values of the corresponding bands.
Emissivity values of band 10 and band 11 are given in the Table 5:

Table 5: Emissivity Values.

Emissivity	Band 10	Band 11
εs	0.971	0.977
εv	0.987	0.989

Step-4:
FVC - Fractional Vegetation Cover was estimated for a pixel. FVC for an image was calculated by following Equation 11:

$$\boldsymbol{FVC} = \frac{(\boldsymbol{NDVI - NDVIs})}{(\boldsymbol{NDVIv - NDVIs})} \quad (11)$$

where,
NDVIs – NDVI reclassified for soil (NDVImin= -1)

NDVIv – NDVI reclassified for vegetation (NDVImax= +1)

The NDVI value often fluctuated between -1 and +1. The NDVI picture was classed into soil and vegetation to get NDVIs and NDVIv; the classified data were then utilized to ascertain FVC. Equation 12 was used to calculate the mean and difference LSE after LSE was generated for both TIR bands.

$$\boldsymbol{\varepsilon} = \frac{\boldsymbol{\varepsilon 10 + \varepsilon 11}}{\boldsymbol{2}} \quad (12)$$

where,
ε – Mean LSE;ε10 and ε11 - LSE of band 10 and 11.

Step-5:
After all of that, we were able to use the SW method to get the LST in Kelvin.

Here, the SplitWindow (SW) algorithm, a structured mathematical approach, was used to compute LST. In order to calculate LST, it takes into account the mean and difference in land surface emissivity, as well as the brightness temperature of two bands of TIR. According to Eq. 13, the LST is determined as follows:

$$LST = TB10 + C1\,(TB10 - TB11) + C2\,(TB10 - TB11)^2 + C0 + (C3 + C4W)(1 - \varepsilon) + (C5 + C6W)\Delta\,\varepsilon \quad (13)$$

where LST denotes the temperature of the land surface in kelvin and C0 to C6 denotes the split-window range Coefficient values The brightness temperatures of bands 10 and 11 are denoted by the notation TB10 and TB11 respectively (K)

The mean LSE of the TIR bands is denoted by, while the amount of water vapor in the atmosphere is denoted by W. (Generally taken as 0.5).

Differences in the values of the LSE and SW coefficients are presented in Table 6 as follows:

Table 6: SW Coefficient Values

Constant	Value
C0	-0.268
C1	1.378
C2	0.183
C3	54.300
C4	-2.238
C5	-129.200
C6	16.400

3. RESULTS AND DISCUSSIONS

In this work, the spatiotemporal pattern of lST is analyzed, and the vegetation health monitoring indices, such as NDVI, SAVI, and MSAVI, are interpreted as indicators of the degradation of the environment. Specifically, the research focuses on the relationship between lST and NDVI. The findings acquired from the bio-thermal analysis carried out at and in the surrounding area of the Rajbandh dump have been segmented into the following parts for the sake of analysis and debate.

Table 7: The Overall Comparison of Temperature of Batiaghata Thana.

Year	Highest Temp (℃)	Lowest Temp (℃)
November 21, 1995	23.00	20.00
Feb 2, 2000	24.00	13.30
November 13, 2005	26.27	21.52
December 10, 2010	21.52	17.04(using Landsat 5)
November 6, 2015,	36.59	27.45(using Landsat 8)
26 Dec,2020	41.43	29.68

3.1 Comparison of Temperatures

All From the reclassified images of 6 year, highest, lowest and average temperatures are obtained which is shown in the Table 7. From an overall comparison of the temperatures of Batiaghata thana beginning in 1995 and continuing through 2020, it can be seen that the highest temperature rises sharply from 23.00 degrees Celsius in the year 1995 to 26.27 degrees Celsius in the year 2005, and then it drops to 21.52 degrees Celsius in the year 2010. Also, the lowest temperature had a sharp increase, going from 20.00 degrees Celsius in 1995 to 21.52 degrees Celsius in 2005, before dropping to 17.04 degrees Celsius in 2010. The average temperature will practically remain the same, climbing to 35.55 degrees Celsius in the year 2020 from 21.5 degrees Celsius in the year 1995. According to the findings of the LST, the highest temperature that has ever been recorded in the Batiaghata thana has risen from 23.00 degrees Celsius in the year 1995 to an ideal temperature of 41.43 degrees Celsius in the year 2020. Figure 3 is a graph that shows a comparison of the greatest, lowest, and average temperatures recorded in Batiaghata thana throughout the course of the years. The reclassified images of LST of 2000 and 2020 are given in the Figure 4 and Figure 5 respectively.

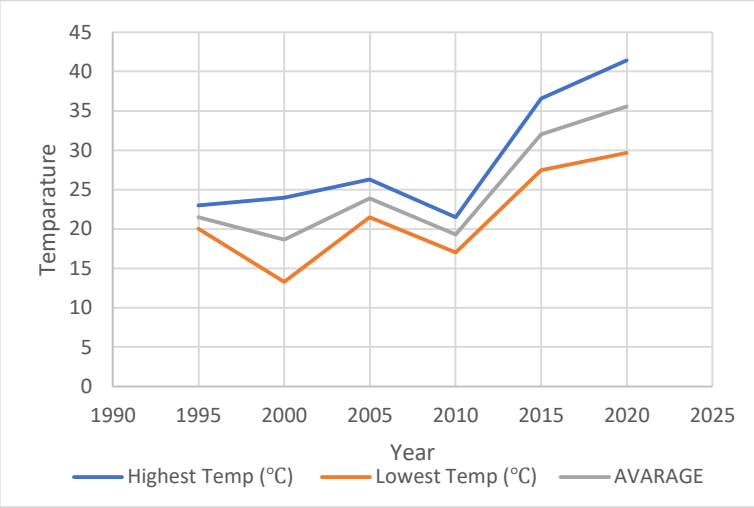

Figure 3: The graph shows the greatest, lowest, and average temperatures recorded in Batiaghata.

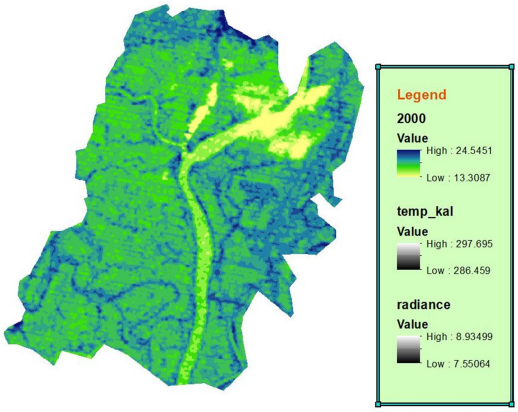

Figure 4: Reclassified LST image of Batiaghata (2000)

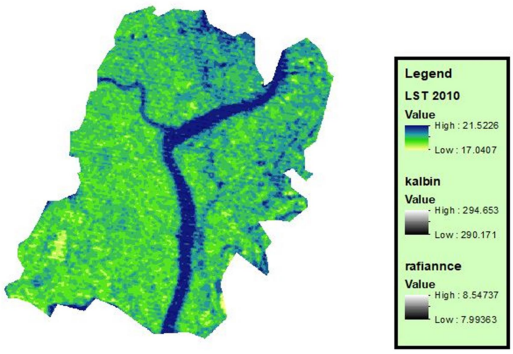

Figure 5: Reclassified LST image of Batiaghata (2010)

3.2 Bio-Indicators

Table 8: The NDVI Pixel Percentage of Each Range Averaged out across the Entire Area (Based on the Pixel Count)

NDVI Category	**Value Range**	**Nov 21, 1995**	**Feb 2, 2000**	**Nov 13, 2005**	**Dec 10, 2010**	**Novr 6, 2015**	**26 Dec,2020**
Water Body	-0.5 - 0	9.935886	8.559508	8.661476	10.31109	7.979427	9.166043
No vegetation	0	0.137558	0.291741	0.42287	1.847569	0.003779	0.003779
Bare Soil	0-0.05	1.207785	0.778103	1.20573	6.795834	4.566583	4.433561
Structural Object	0.05-0.1	1.256157	1.154872	1.793703	20.63692	23.06192	13.27763
Shrub and Grassland	0.1-0.3	13.39183	9.21706	16.36249	60.21132	63.68879	73.05625
Moderate Vegetation	0.3-0.6	73.989324	70.32742	68.85717	0.197266	0.699499	0.062732
High Vegetation	0.6-0.8	0.082005	9.6713				

The NDVI Pixel Percentage of Each Range Averaged out across the Entire Area Table 8 presents the results (Determined by the Number of Pixels) It was discovered that the proportion of pixels in the "water body" category ranged from a low of 7.97% in the year 2015 to a high of 10.31% in the year 2010. The percentage of pixels in the Structural Object category ranged from a low of 1.95 percent in 2005 to a high of 23.06192 percent in 2015. In the category of Shrub and Grassland, the proportion of pixels ranged from a low of 9.21% in the year 2000 to a high of 73.56% in the year 2020. The proportion that falls under the Bare Soil category ranged from 0.7 to 1.20% up until the year 2005. In 2010, it increased by a significant margin of 6.79% over the previous year. The category known as Moderate Vegetation displays a percentage that ranges from 73.98 to 68.85% during the first 10 years. After another 10 years, it will have dropped to 0.69 percent, and then it will be gone entirely in 2020.

Figure 6 presents a visual representation of a comparison between the Bare Soil, Shrub, and Grassland of Batiaghata thana for one year. The reclassified images of NDVI of 2000 and 2020 are given in Figure 7 and Firgure 8 respectively.

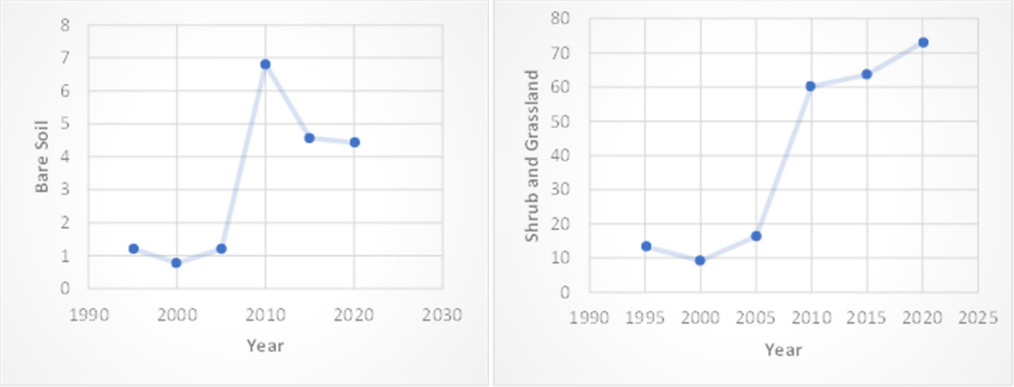

Figure 6: The graphical comparison of the Bare Soil and Shrub and Grass land of Batiaghata

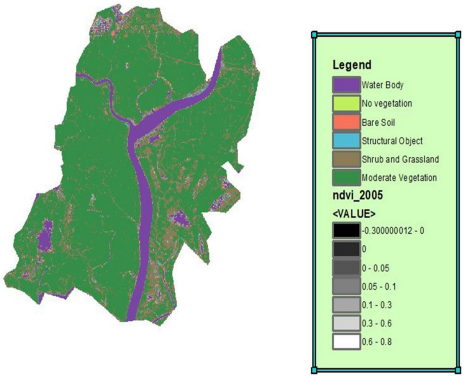

Figure 7: Reclassified NDVI image of Batiaghata (2005)

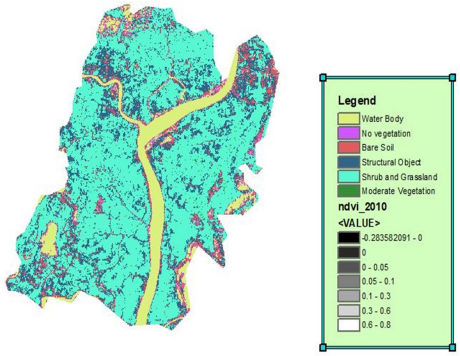

Figure 8: Reclassified NDVI image of Batiaghata (2010)

3.3 SAVI

Table 9: The Overall Comparison of SAVI of Batiaghata Thana.

YEAR	MAX VALUE	MIN VALUE
1995	0.93	-0.55
2000	1.17	-.066
2005	0.89	-0.44
2010	0.56	-0.42
2015	0.61	-0.15
2020	0.55	-0.18

The images of SAVI of 2005 and 2020 is shown in Figure 9 and Figure 10, respectively. The graphical comparisons of the highest and lowest value of SAVI are given in the Figure 11.

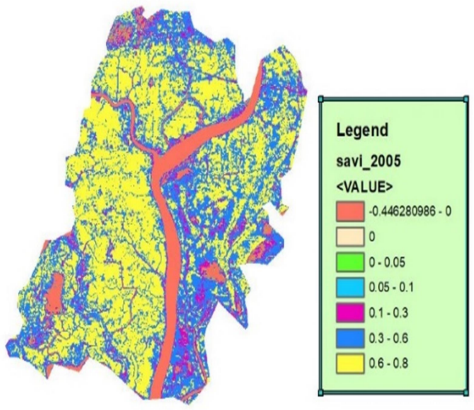

Figure 9: Reclassified SAVI image of Batiaghata (2005)

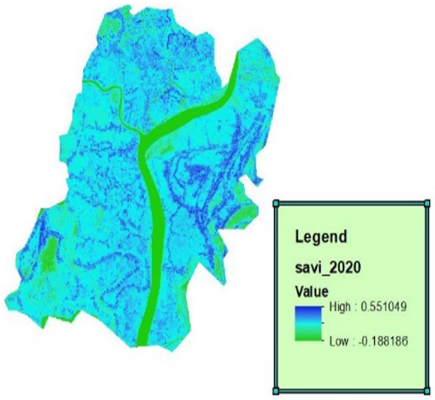

Figure 10: Reclassified SAVI image of Batiaghata (2020)

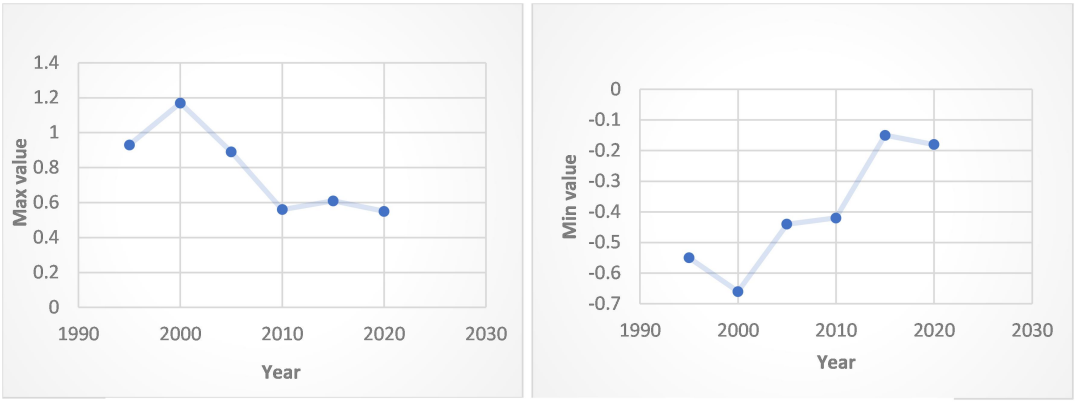

Figure 11:The graphical comparisons of the highest and lowest value of SAVI.

Figure 11 is a visual depiction of the comparisons between the highest and lowest temperatures that were recorded in the chosen location. The visual comparison that was just presented shows that the greatest value of SAVI grew from 0.93 in 1995 to 1.17 in 2000. This is something that can be seen. After reaching its highest position, it began falling until it reached 0.55 in the year 2020. Because a positive number that is greater indicates healthy vegetation and a positive value that is lower indicates unhealthy vegetation, one may conclude that the growth of the vegetation has decreased significantly. The lowest value of SAVI dropped from a value of -0.55 in 1995 to a value of -0.66 in 2000, as seen in the visual comparison presented earlier in this section. From the time where it was at its best, it dramatically declined to -0.15 in 2015. The water body is represented by the negative value in this case.

3.4 MSAVI

Table 10: the Overall Comparison of MSAVI of Batiaghata Thana.

YEAR	MAX VALUE	MIN VALUE
1995	0.76	-1.12
2000	0.80	-1.5
2005	0.76	-0.82
2010	0.65	-0.5
2015	0.58	-0.23
2020	0.537	-0.28

Table 10 is an illustration of the overall comparison of the MSAVI of Batiaghata thana at several selected years. It was noticed that the greatest value of MSAVI was growing from 0.76 in 1995 to 0.80 in 2000. This trend continued from 1995 to 2000. After reaching its highest position, it began falling until it reached 0.537 in the year 2020. Because a positive number that is greater than zero shows healthy vegetation and a positive value that is lower than zero reflects bad vegetation, one may conclude that the growth of the vegetation has been significantly stunted. It has been observed that the value of MSAVI that is lowest has been becoming lower with time, going from -1.12 in 1995 to -1.5 in 2000. From the moment where it was at its best, it has dramatically declined to -0.23 in 2015. A negative number denotes the presence of water in this context. Because the graph only displays the lowest and highest possible values, it is impossible to determine whether the water body has increased or decreased in size over the course of this specific year.

4. CONCLUSIONS

It can be shown from an overall comparison of the temperatures of Batiaghata thana beginning in 1995 and continuing through 2020 that the maximum temperature rose sharply over the course of that time period, going from 23.00 degrees Celsius in 1995 to 41.43 degrees Celsius in 2020. In addition, the lowest temperature will skyrocket, going from 20.00 degrees Celsius in 1995 to 29.68 degrees Celsius in 2020.The temperature rises at and around Rajbandh landfill mainly due to the waste decomposition process. But in the Batiaghata thana area, there are various reasons for urbanization, industrial activity, deforestation, etc. except the waste decomposition process. Because of rapid urbanization and industrialization, solid waste disposal in the surrounding environment has increased significantly. The operational activities of Rajbandh landfill started in 1984, so the temperature is relatively more minor as any industrial activities or other temperature increasing activities did not happen at and around the landfill site in 1995. With the starting of these activities, the place has turned into a Semi-aerobic landfill from barren land. According to the findings of the study, as soon as activities at the dump began, the temperature in and near Rajbandh landfill quickly soared, going from a range of 20-22 degrees Celsius to 40-42 degrees Celsius. Because the graph only displays the lowest and highest possible values, it is impossible to determine whether the body of water has increased or decreased in size throughout the course of this specific year.

REFERENCES

Range of output value of NDVI. (2019, March 13). Retrieved from https://phenology.cr.usgs.gov/: https://phenology.cr.usgs.gov/

Bannari, A. M. (1995). A review of vegetation indices. Remote Sensing Reviews, Vol. 13, No. 1, pp: 95 - 120.

Danthurebandara M., P. S. (2012). ENVIRONMENTAL AND SOCIO-ECONOMIC IMPACTS OF LANDFILLS. Linnaeus ECO-TECH, (p. 13). Kalmar, Sweden.

Huete, A. R. (1988). A soil-adjusted vegetation index (SAVI). Remote Sens. Environment, Vol. 25, pp: 295-309.

Interpretation of NDVI . (2019, March 13). Retrieved from https://earthobservatory.nasa.gov/features/: https://earthobservatory.nasa.gov/features/

J. Qi, A. C. (1994). A Modified Soil Adjusted Vegetation Index. Remote Sens. Environment, Vol. 48, pp: 119-126.

Jiang Z., H. A. (2007). Interpretation of the modified soiladjusted vegetation index isolines in red-NIR reflectance space. Journal of Applied Remote Sensing, Vol. 1, No. 1.

Kawai, K. a. (2016). Revisiting estimates of municipal solid waste generation per. Journal of material Cycles and Waste Management., 18(1), 1-13.

Population of Bangladesh. (2019, March 18). Retrieved from worldpopulationreview.com: http://worldpopulationreview.com

Population of Bangladesh. (2019, March 18). Retrieved from bbs.gov.bd/: http://www.bbs.gov.bd/

Rafizul, I. a. (2019). Spatiality, seasonality and index analysis of heavy metals in soil of waste disposal site in Khulna of Bangladesh. Journal of Solid Waste Technology and Management, vol. 45, issue 2, pp. 234-256.

Song Z., L. R. (2018). Global Land Surface Temperature Inuenced by Vegetation Cover and PM2.5 from 2001 to 2016. Remote Sens. Environment, Vol. 10, No. 2034.

This paper is the extended version of the conference paper presented in ICCESD 2022.